

Article

# Geovisualization of the Excavation Process in the Lesvos Petrified Forest, Greece Using Augmented Reality

Ermioni-Eirini Papadopoulou <sup>1</sup>, Vlasios Kasapakis <sup>2</sup>, Christos Vasilakos <sup>1,\*</sup> ,  
Apostolos Papakonstantinou <sup>3</sup>, Nikolaos Zouros <sup>1</sup>, Athanasia Chroni <sup>1</sup> and Nikolaos Soulakellis <sup>1</sup>

<sup>1</sup> Department of Geography, University of the Aegean, 81100 Mytilene, Greece; epapa@geo.aegean.gr (E.-E.P.); nzour@aegean.gr (N.Z.); geom18020@geo.aegean.gr (A.C.); nsoul@aegean.gr (N.S.)

<sup>2</sup> Department of Cultural Technology and Communication, University of the Aegean, 81100 Mytilene, Greece; v.kasapakis@aegean.gr

<sup>3</sup> Department of Marine Sciences, University of the Aegean, 81100 Mytilene, Greece; apapak@aegean.gr

\* Correspondence: chvas@aegean.gr; Tel.: +30-22510-36451

Received: 14 May 2020; Accepted: 5 June 2020; Published: 7 June 2020



**Abstract:** Augmented reality (AR), in conjunction with 3D geovisualization methods, can provide significant support in monitoring geoconservation activities in protected geosites, such as the excavation process in fossil sites. The excavation process requires a monitoring methodology that will provide a complete and accurate overview of the fossils, their dimensions, and location within the different pyroclastic horizons, and the progress of the excavation works. The main purpose of this paper is the development of a user-friendly augmented map application, specifically designed for tracking the position of petrified tree trunks, providing information for their geometric features, and mapping the spatiotemporal changes occurring in the surrounding space. It also aims to probe whether the rapid acquisition of a 4K video can generate cartographic derivatives of petrified findings during a geosite excavation. A database accumulated 2D and 3D cartographic information, while the geovisualization environment displayed the surface alterations, at two scales: a) 1:500 (excavation area) and b) 1:50 (trench level). Unmanned aerial systems (UASs), used for data acquisition in three excavation periods, consisted of two flights at two different altitudes: one to record changes throughout the study area and the other to provide information on trunks at trench level, via a high-resolution (4K) video. Image-based 3D modeling followed, in which image georeferencing was conducted with ground control points (GCPs). Finally, 2D and 3D geovisualizations were created to depict the excavation changes through time. The cartographic products generated at two cartographic scales depicted the spatiotemporal changes of the excavation.

**Keywords:** augmented maps; 3D geovisualization; petrified tree trunks; unmanned aerial system (UAS)

## 1. Introduction

Three-dimensional cartography is a combination of science, aesthetics, and technical knowledge and activities related to all stages of building 3D maps, such as data collection, production and distribution processes, fundamental technologies and algorithms, and the final context of application [1]. Digital tools, such as geographic information systems (GIS) and augmented reality (AR), have played an important role in developing new methods of processing and visualizing spatial information, in addition to evaluating and mapping them, enabling the growth of new ways of highlighting and preserving geoheritage. Recently, the development of new digital technologies has strongly influenced scientific practices in the field of geoheritage [2,3]. Good practices have been observed regarding 3D

visualization in various areas, such as the study and preservation of cultural heritage, in addition to visualization and dissemination of this information over the Internet [4].

Another development that has enhanced the science of photogrammetry and the data acquisition process is the appearance of unmanned aerial systems (UASs). UASs have become precious tools for generating spatial data for various geoscientific analyses [5]. The most common applications of UASs pertain to the acquisition and processing of aerial photography using photogrammetric methods for making orthophotomaps, digital surface models (DSMs), and 3D models [6]. Accurate positioning is achieved, in many cases, through the use of fixed terrestrial control points and real-time kinematic technology, which assists monitoring of a particular area and collection of spatiotemporal data [7]. Simultaneously, the evolution of technology has also led to the development of image processing algorithms and computer visualization. One popular algorithm is structure from motion (SfM) [8] and the methodology of image-based 3D modeling [9].

Some authors have also suggested that SfM and stereo matching are useful for documentation and excavation monitoring [10,11]. An efficient implementation of these approaches was demonstrated during the excavation process at the Upper Palaeolithic of Shuidonggou Locality 2 site in China in 2017 [11]. The outcome of this research showed that SfM photogrammetry can support the documentation of the findings with sufficient accuracy for analytical purposes and enhances the logistics of the excavation process. In addition, in a study of geomorphological mapping of granite tors in Poland, it was shown that the use of the SfM algorithm is appropriate for mapping rocks and rocky areas, and concluded that the approach allows the recognition of micro-topography [12]. In a study by Hoon et al. [13], laser scanning and photogrammetry were combined in order to produce integrated documentation of a cultural heritage site. Overall, the SfM algorithm can help in geophysical measurements of the geometry of similar areas.

The evolution of technology beyond the means of data collection and processing has greatly influenced the visualization of geospatial information. Augmented reality (AR) is the overlay of graphic digital information on real-world images. Its main purpose is to combine real-world and virtual information, in conjunction with providing real-time interaction for users [14,15]. More precisely, users experience an illusion with regard to the real world as they receive additional information (e.g., images, sounds, and text). However, extended research has demonstrated that spatial information adds more plausibility to the enhanced environment than any other information, assisting users in several scientific issues [16]. For instance, a number of studies have proposed applications of simulation, which have used different features, such as representations by 3D models, web interfaces, and AR virtual tours in interior [17] and outdoor environments [18]. In the European Association for the Protection of Geological Heritage (PROGEO-Piemonte) project, virtual tours were developed of the geoheritage of the region, with the purpose of diffusing geological knowledge and raising people's awareness of geodiversity and earth sciences [19]. An AR application was developed using images converted to 3D animation of four volcanic geoheritage sites in Czech Republic, increasing a young audience's interest in geoheritage matters [20]. Augmented reality techniques were used for developing an application that enables the end-user to value six known geological sites located in Castilla y León, Spain. Geomatic resources were generated, offering real-time interaction with cartographic products, such as thematic maps and digital terrain models. Thus, the authors proposed a virtual route in Google Earth and a detailed field trip guide for educational purposes [21].

Some researchers have driven the further development of computer visualization of geoheritage, integrating UASs for data capture and using multimedia technologies for delivering content. More specifically, Santos et al. [2] blended panoramic photos of 3D representations, videos, text information, sound, and images in an AR application in 2018. Several studies have recognized the dual use of AR. On one hand, AR is applied in the field of heritage for the promotion of an area; on the other hand, there are some studies using this tool for site management. It has been reported in a study that AR applications can support monitoring and documentation of construction site progress [22], while a

recent study by Koo et al. [23] concluded that a further step could be the integration of a free wireless link, databases, and cloud computing into AR applications.

AR tools, in conjunction with UAS data collection and 3D geovisualization methods, can provide significant support for monitoring excavation processes. This study aims to explore whether the rapid acquisition of a 4K video can produce cartographic products of petrified findings during a geosite excavation. Our final goal is to develop an AR application for monitoring two parallel processes: (a) the dismantling of wind turbines and the installation of new ones and (b) the excavation works of fossil trunks at the Acroheiras Wind Park on Lesbos island, Greece. As the exposure and recording of this kind of finding requires special handling and must take place under great caution, the surveillance of excavation works is considered necessary. To our knowledge, no prior application has been developed capable of following two interrelated procedures that serve different purposes. In the proposed approach, the end-user can quickly access useful information for trunks' geometric features through a device, as well as see the changes occurring in the surrounding space. There are two display options of the environment; either the whole excavation area or the trench, where the trunks are placed. The geovisualization of data, obtained by a 4K video, is represented at two scales: (a) 1:500 (excavation area) and (b) 1:50 (trench level). The first cartographic scale is needed for observing the geosite's surface alterations; the second allows recording of the exact location of trunks and the depth at which they are discovered, while collecting useful information about their size, orientation, and incline. The combination of augmented maps, composited from both scales, creates a useful application for excavation monitoring or visualizing petrified tree trunk features.

## 2. Materials and Methods

### 2.1. Study Area

The Lesbos Petrified Forest is located on the western peninsula of Lesbos island, in the northeast Aegean Sea, Greece. It represents a rare fossilized forest ecosystem that contains fossiliferous locations with large concentrations of petrified trees and fossil animals covered by pyroclastic materials, and was fossilized in situ 18 million years ago [24–26]. Standing and falling petrified tree trunks, branches, roots, fruits, and leaves of trees, as well as animal bones and teeth, have been found within layers of volcanic ash. Significant fossil-bearing localities have been also found both at the coastal zone and the marine area to the west of Lesbos, adjacent to impressive outcrops that border the petrified forest area, evincing intense volcanic activity in the past. The Lesbos Petrified Forest was declared a protected monument of nature in 1985, covering an area of 15,000 ha. Due to its international scientific importance and value, Lesbos island was recognized as a UNESCO Global Geopark.

Wind potential on the western peninsula of Lesbos island is high. Thus, the Acroheiras wind-mill park of nine wind turbines was established in the 1990s and is located within the protected area of the Lesbos Petrified Forest (Figure 1). In 2018, the process of replacement of the wind turbines began. However, the new turbines were larger than the previous ones, so the expansion of their bases was considered essential. The excavation process was suspended, however, when fossilized trunks were discovered. Due to the protected status of the area, a series of procedures have been followed during excavation works. These procedures aimed to document the findings and the detailed monitoring of the overall process.

Rescue excavations were conducted by the Natural History Museum of the Lesbos Petrified Forest. During the excavation works, several petrified trees were unearthed. The excavation process requires detailed monitoring, which provides a complete and accurate overview of the fossils, their dimensions, and their location within the different pyroclastic horizons at the different stages of the excavation works. To achieve better results, an advanced methodology was developed for recording the findings and monitoring the overall process.



**Figure 1.** Location of the study area, Acroheiras site, Lesvos Petrified Forest, Lesvos, Greece (Sources: Esri, DigitalGlobe, GeoEye, i-cubed, United States Department of Agriculture Farm Service Agency (USDA FSA), United States Geological Survey (USGS), Aerial Express (AEX), Getmapping, Aerogrid, Instituto Geográfico Nacional (IGN), swisstopo, and the Geographic Information System (GIS) User Community, General Bathymetric Chart of the Oceans (GEBCO), National Oceanic and Atmospheric Administration (NOAA), National Geographic, DeLorme, HERE, Geonames.org, and other contributors).

2.2. Methodology

The methodology used combines the fundamentals of classic cartography, image-based 3D modeling, computer vision algorithms, and AR techniques. Figure 2 presents the three steps of the methodology [27]: (a) data acquisition, (b) data processing, and (c) 3D geovisualization implementation.

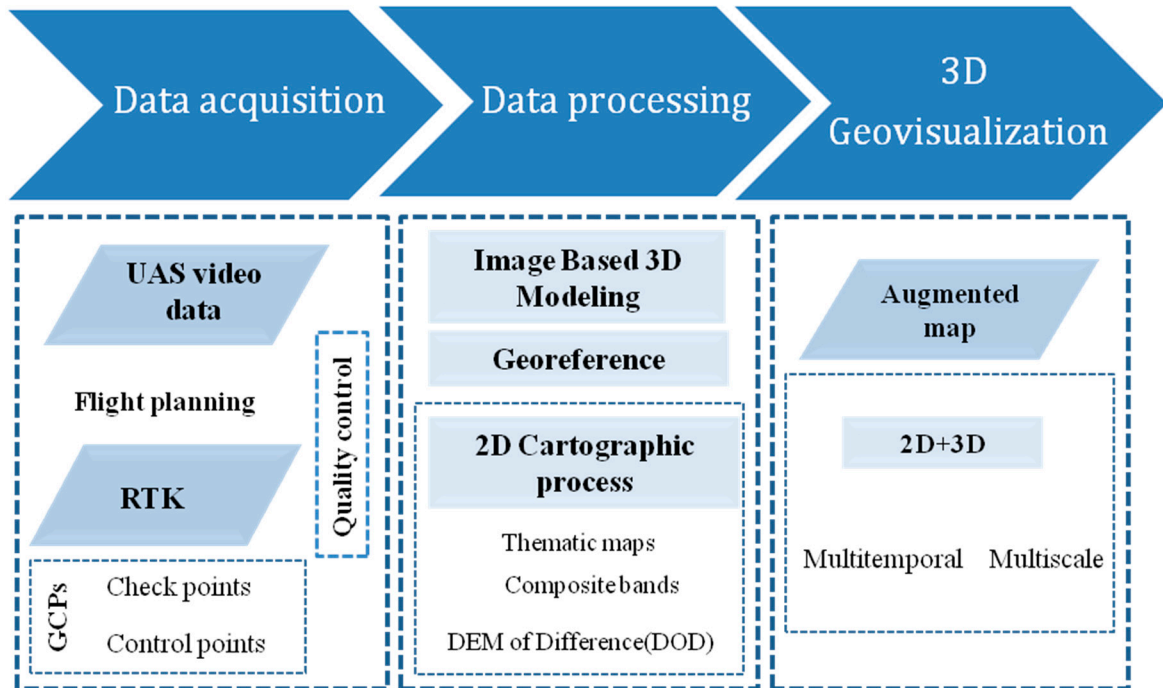


**Figure 2.** Methodology pipeline.

### 3. Data Acquisition

#### 3.1. UAS Data Collection

The data acquisition process took place at three temporal periods (01 August 2018, 07 October 2018, and 11 November 2018). Two distinct flights were designed at two different altitudes, mainly for documenting the changes across the study area, and also for gathering information for petrified tree trunks at trench level. The aerial platform used for data acquisition was the DJI Phantom 4 Pro quadro-copter. UAS-based methods usually suffer from a number of limitations. Legislative limits, dense vegetation, steep slopes, shadows, and high elevation structures frequently influence UAS surveys. In the present study, strong winds were the factor that most affected our flights, thus no flight was performed during September of 2018. Table 1 presents the flight plan information and camera specifications. The flight plans were created having two different heights to respond to the need for mapping at the two preselected cartographic scales. The combination of the flight path pattern (parallel lines) and the means of data collection (4K video) delivered an adequate set of data, without needing terrestrial image capture. In addition, the angle of the camera was set vertical to the ground; there were no blind areas, as the surface of the study area does not have steep slopes and high vegetation. The protected area of the Lesvos Petrified Forest constitutes a site of great findings for geoheritage and the avoidance of landscape changes is important for the competent management body. The first mission was designed with a spatial extent covering the entire wind park to provide an overview of the current state of the study area, including all nine sites from which the wind turbines were moved. Subsequently, separate flights at lower altitude were made above the new selected turbine positions, indicated by the site's managers. The cartographic scales that were used for the visualization of the collected data for the (a) excavation area and (b) trench level (site) were 1:500 and 1:50, respectively. The 1:500 cartographic scale ensured the oversight of the whole excavation area. Mapping at a larger scale (1:50) helped us to monitor the findings closely, as it was important to record geometric features of the petrified tree trunks, as well as their position.

**Table 1.** Flight plan information and camera's specifications.

Date	01 August 2018	07 October 2018		11 November 2018	
Study Area	Excavation Area	Excavation Area	Trench Level (Site)	Excavation Area	Trench Level (Site)
Height of flight	50 m	50 m	20 m	50 m	20 m
Time of flight	11:30 a.m.	11:45 p.m.	12:30 p.m.	12:00 p.m.	12:45 p.m.
Duration	19 m	19 m	11 m	19 m	11 m
Total Distance	4800 m	4800 m	1300 m	4800 m	1300 m
Ground Sampling Distance (GSD)	0.06 m	0.06 m	0.02 m	0.06 m	0.02 m
Speed			15 km/h		
Gimbal Pitch			Vertical		
Heading			To the next way point		
Sensor specs	Resolution: 24.3 MP, width: 6.3 mm, height 4.7 mm, focal length 19 mm 1.55 $\mu$ m sensor pixel size				

During the first flight plan, the flight altitude was set at 50 m and the collected data consisted of a 4K video. The choice between recording video over taking photos for our data collection was endorsed by the dynamic nature of excavation works. Although the area covered by a UAS flight is the same regardless of the means of recording, the choice of using 4K video was supported by the need to acquire as much information as possible during a flight. The advantage of the 4K video recording is that it captures 59 frames per second (fps). The ground sampling distance (GSD) of the video was calculated according to the height parameter and the camera's sensor specifications. The side overlap was fixed at 60%, while the front overlap was defined at a later stage during frame extraction. High resolution of data was achieved by setting the flight altitude to 20 m with side overlap 60%, in order to thoroughly map the morphological features of petrified tree trunks.

The data acquisition flight for all three dates had the same flight characteristics to achieve the maximum comparability between the datasets collected. At the first date of monitoring, only one flight at 50 m was made for the general surveillance of the area, as no findings had been reported. Thus, the need for lower and larger spatial resolution data had not occurred yet.

### 3.2. Real-Time Kinematic Data Collection

Georeferencing of the project's outputs was supported by real-time kinematic (RTK) measurements. The geometry of the study area was relatively irregular and, due to the nature of the terrain, the location of the points had to be carefully selected. Due to multitemporal acquisitions, 36 ground control points (GCPs) were carefully selected in order to be identifiable, while a station of the Greek reference network was used as the base (Figure 3). Five of the GCPs were used for georeferencing of the project and the remainder were used as check points of the excavation area (scale 1:500), whereas for the trench level (scale 1:50), the number of points was 4 and 32, respectively.

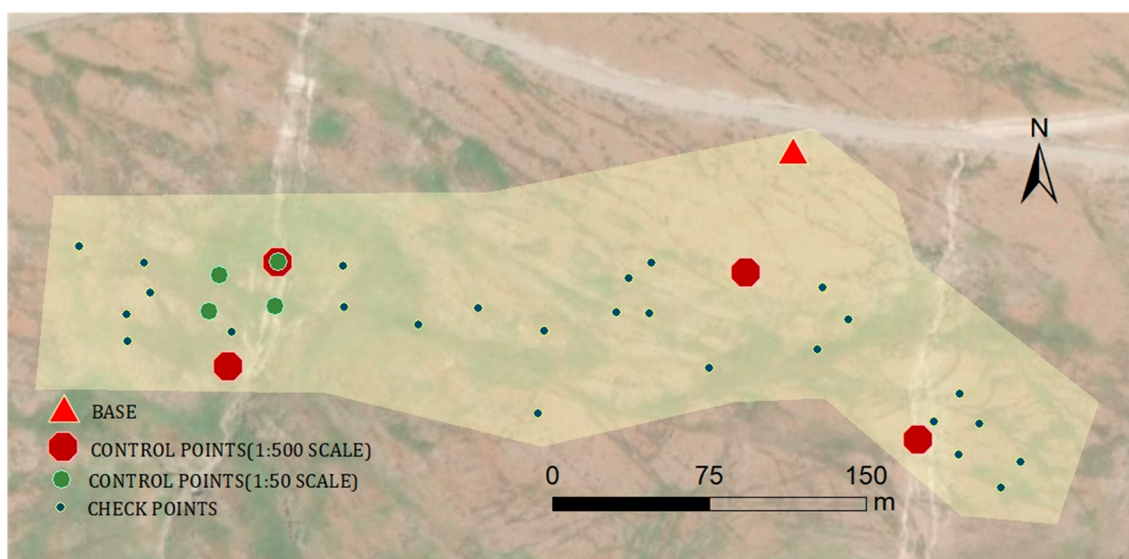


**Figure 3.** Distribution of control and check points at the study area.

## 4. Data Processing

### 4.1. Image-Based 3D Modeling

The image-based 3D modeling process consisted of eight stages as shown in Figure 4. The first step in data processing was the frame extraction from the ultra-high resolution 4K video. The requirement of parallax was fulfilled by setting the front overlap above 80%. The frame extraction was set to one frame per second, which was calculated by the UAS's velocity (15 km/h), in order to achieve the desirable overlap. A set of 689 photos, with  $4096 \times 2160$  pixel resolution, was extracted from the video for the entire case study area, while the number of photos extracted for the site area was 256 with the same resolution. The same procedure was followed for three different study dates.

Quality control of images, resulting from frame extraction, was done visually and through the Image Quality Index of Agisoft Photoscan [28]. The images were checked individually, and were categorized as suitable or unsuitable for editing. Blurry, overloaded, or noisy images were considered unsuitable for further processing. The structure from motion algorithm was then applied to every dataset for each date and scale. The sparse point cloud resulting from SfM was georeferenced by RTK measurements. In order to increase the density of the georeferenced 3D point cloud, the multi-stereo view algorithm was applied. The output was a dense point cloud, which was used to create a 3D mesh. Finally, the DSM and the orthophotomap were produced.

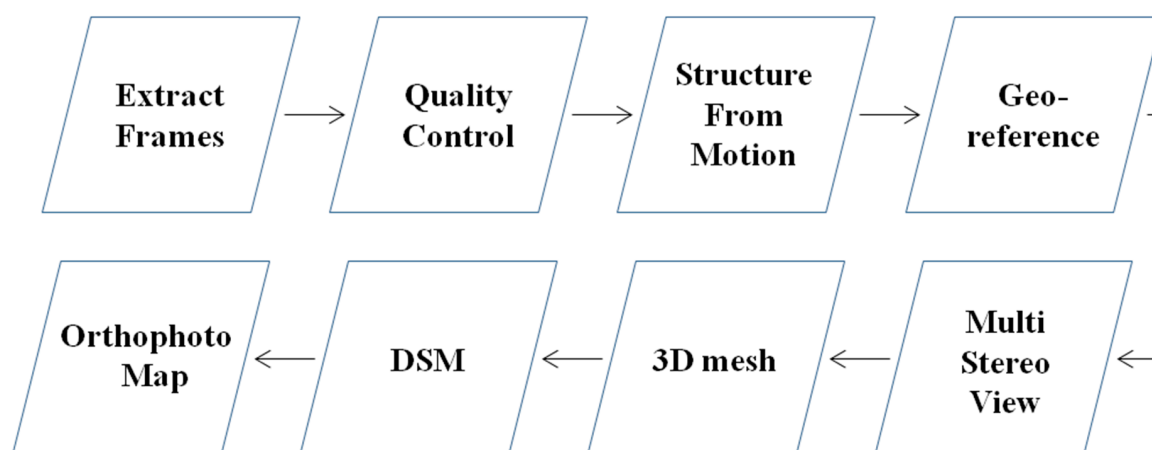


**Figure 4.** Image-based 3D modeling stages.

A total of five 3D georeferenced point clouds were created on the three recording dates (01 August 2018, 07 October 2018, and 11 November 2018) and at two cartographic scales: a) overall excavation area and b) trench level (site). The total root mean square error (RMSE) of the control points for the first recording date was 6.1 cm for both cartographic scales (Table 2). On the second date of recording, the RMSE was 6.4 cm for the 1:500 scale and 2.4 cm for the 1:50 scale. The total RMSE for the third date was 5.0 cm (1:500) and 4.9 (1:50). The point cloud that was created on the first recording date (01 August 2018) was from a flight height of 50 m, representing the entire study area before the excavation process began. The first 3D dense point cloud (Figure 5a) shows the six trenches, corresponding to the six locations where wind turbines were located prior to their removal. On this date, there were no findings (petrified tree trunk) in the trenches, as there was no indication of any possible petrified tracing sites. At the trench level shown in Figure 5b, the first wind turbine installation location is presented. This segment is part of the original point cloud, which was isolated and processed. The next acquisition took place when the installation project was significantly progressed. At the excavation area level, Figure 5c displays the entire excavation area, and it can be observed that some parts of the former wind turbine bases had been excavated. At the second level, on the same date (Figure 5d), a petrified tree trunk appears in the first point of installation of a new wind turbine. On the third acquisition date (11 November 2018), there are intense excavation activities at the trench level (Figure 5e). The fact that the geometry of the trench deviates from the remaining locations that were plotted on the map indicates that new findings appeared at this location. Examining the 3D dense point cloud on 11 November 2018 (Figure 5f) at the trench scale, it is observed that petrified tree trunks emerged from different levels and different directions.

**Table 2.** Total root mean square error (RMSE) of the georeferencing procedure for each acquisition date.

Date	01 August 2018		07 October 2018		11 November 2018	
Scale	1:500	1:50	1:500	1:50	1:500	1:50
RMSE of control points (cm)	6.1	6.1	6.4	2.4	5.0	4.9
RMSE of check points (cm)	3.9	3.9	4.6	3.9	3.0	1.3

Six 3D meshes were created on the three recording dates and at two scales: a) excavation area (1:500) and b) trench level (1:50). The 3D meshes of the excavation area consisted of 1,104,580 faces (01 August 2018), 882,008 faces (07 October 2018), and 573,489 faces (11 November 2018). On the other hand, the 3D meshes generated for the trench level consisted of 19,999 faces (01 August 2018), 573,489 faces (07 October 2018), and 305,319 faces (11 November 2018). The advantage of 3D models is that they are used as a cartographic product both for photorealistic visualization of the situation and for obtaining geometric information about the petrified tree trunks. Combined with the georeferencing

of the 3D models, it is possible to measure the volume of findings and the area excavated, and to derive the overall model.

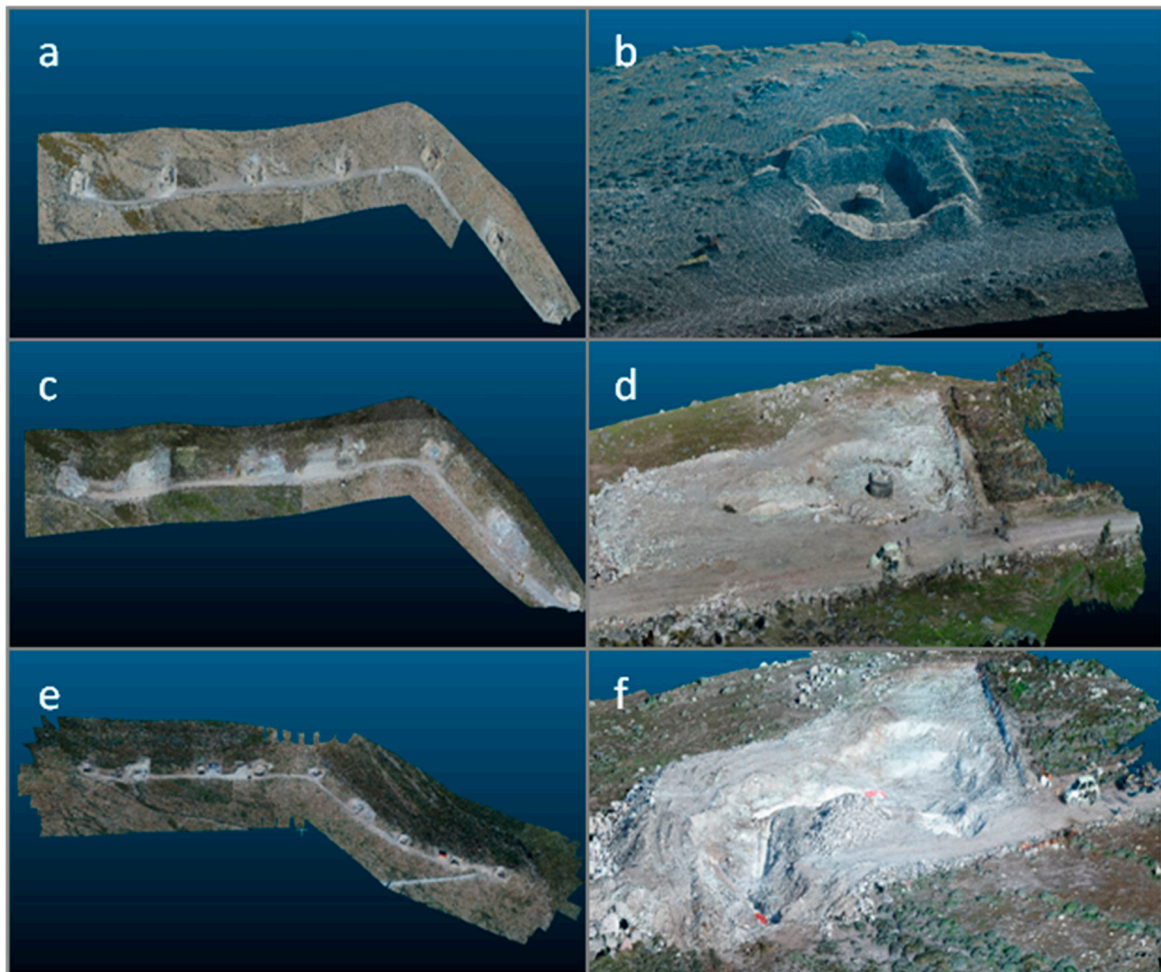


**Figure 5.** Three-dimensional point cloud: of excavation area, (a) (01 August 2018), (c) (07 October 2018), (e) (11 November 2018), and of trench level (b) (01 August 2018), (d) (07 October 2018), (f) (11 November 2018).

Figure 6a,c,e represents the resulting DSMs of the entire study area for the three dates. The highest altitude is 369 m and the minimum 314 m. The highest elevation appears at the northeast of the area near the fifth wind turbine site. This time series of the DSMs reveals the alterations in the surface, i.e., the excavations and the excavation soil deposits. At the largest cartographic scale of the first date (Figure 6b), at the first site the base of the pre-existing wind turbine and the deposits around the trench are depicted. Furthermore, the DSM in Figure 6d has lower elevation values around the base than the DSM in Figure 6b. This indicates that excavation work had been carried out in this section, as a fossil trunk appeared perpendicular to the west side of the trench at an altitude of 350 m. In Figure 6f, three additional petrified tree trunks are observed, to the west of the first trunk. It is worth noting that each trunk lays in a different direction from the others, while to the south of the base, there is a cluster of smaller inferior trunks.

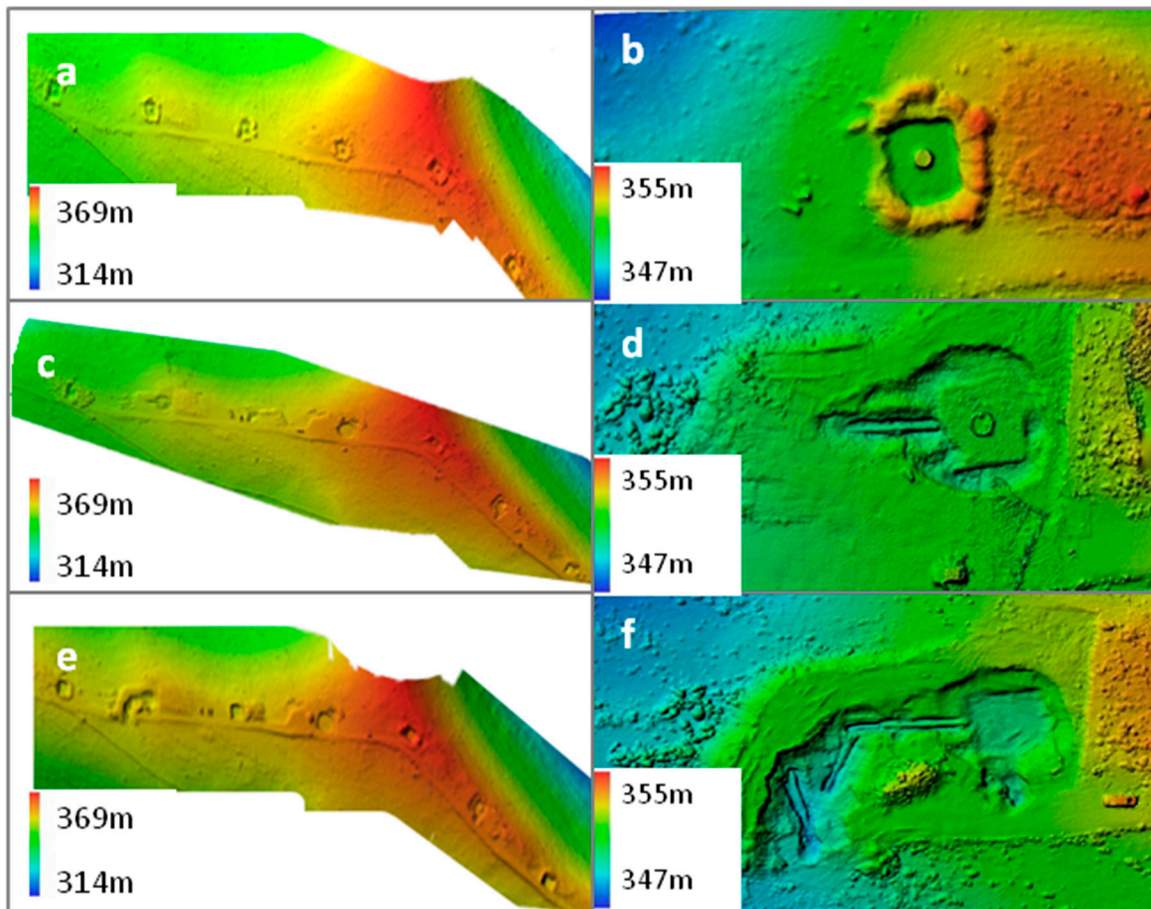


**Figure 6.** Digital surface model (DSM): of excavation area, (a) (01 August 2018), (c) (07 October 2018), (e) (11 November 2018), and of trench level (b) (01 August 2018), (d) (07 October 2018), (f) (11 November 2018).

Six orthophotomaps were created on the three acquisition dates and at two mapping scales. The orthophotomap in Figure 7a presents the entire study area at 1:500 scale and its spatial resolution is 2 cm. The map shows the six bases of wind turbines of the wind park. Figure 7c shows, at 1:500 cartographic scale, the entire study area at 2 cm spatial resolution on the second acquisition date. In particular, there are changes in three of the six wind turbine bases compared to the previous date. Moreover, the largest finding can be observed at the first site. The orthophotomap in Figure 7e captures the entire study area at 1:500 scale and 2 cm spatial resolution on the third recording date. Changes occurred at two of the three bases.

Figure 7b depicts the first location of the new wind turbine on the first recording date, at 1:50 scale and spatial resolution of 2 cm. There is no appearance of petrified trees trunks. The spatial resolution of the map in Figure 7d is smaller than 1 cm and its cartographic scale is 1:50, and a petrified tree trunk is observed with a length of 9.7 m and a width of 0.4 m. The orthophotomap of Figure 7f shows three new fossilized logs: a) 3.8 m long, 0.3 m wide; b) 9.6 m long, 0.7 m wide; and c) 11 m long, 0.6 m wide.

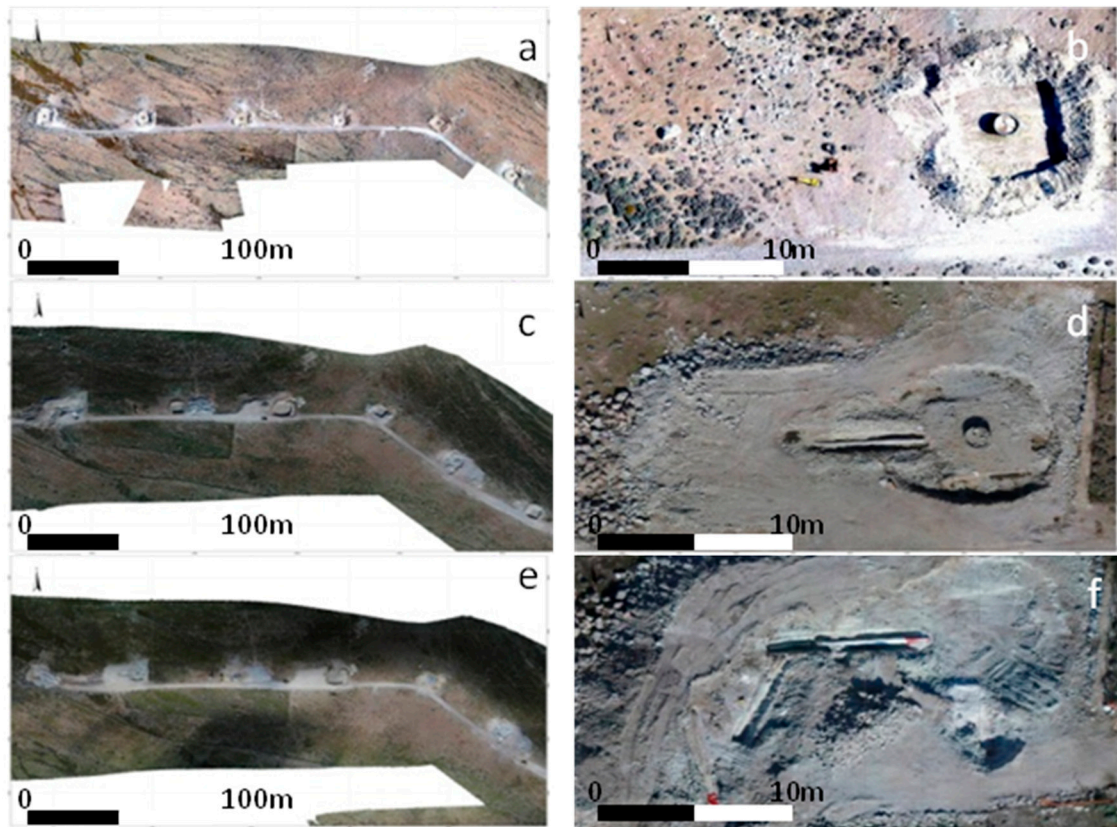


**Figure 7.** Orthophotomap of excavation area, (a) (01 August 2018), (c) (07 October 2018), (e) (11 November 2018), and of trench level (b) (01 August 2018), (d) (07 October 2018), (f) (11 November 2018).

#### 4.2. Cartographic Process

Cartographic methods were used to produce the thematic map of changes that occurred during the excavation process. Polygons were delineated around each excavation trench for each date. The surrounding surface of each trench was calculated, and the number of fossils was determined. Figure 8 represents a thematic map of the whole study area at 1:1000 mapping scale, divided into two parts. The upper part of the map shows the first three sites, while the lower portion shows the remaining sites. The total excavated surface on 01 August 2018 was 570,003 m<sup>2</sup>. On this date, no intense excavation activities were noticed, nor were any petrified tree trunks discovered. Between the first and the second acquisition date, excavations took place at the three bases on which the new wind turbines were to be installed. One trunk emerged at site 1, whilst six trunks were revealed at sites 2 and 3 (three trunks at each site). The total excavated area until the 7th of October 2018 was 1,688,287 m<sup>2</sup>. During the third period, only the first site was further excavated, where three more petrified tree trunks were discovered. The total area excavated on the third recording date (11 November 2018) was 853 m<sup>2</sup>.

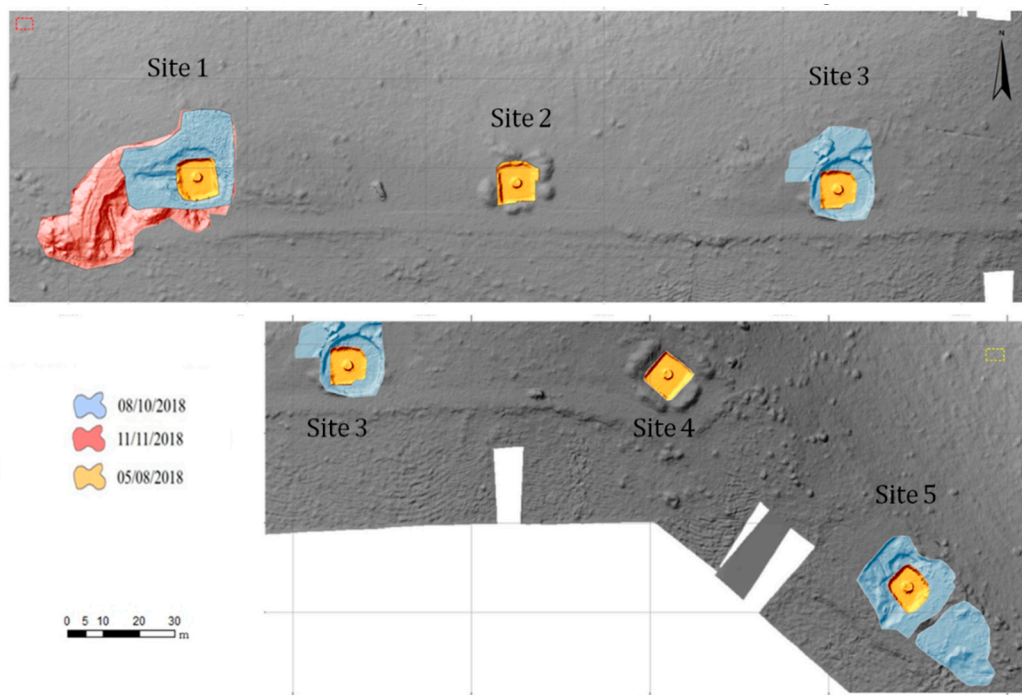


**Figure 8.** Thematic map depicting spatiotemporal changes of the study area.

A series of maps was then created by DSM of difference (DoD). Firstly, the difference between the values in the raster cells was calculated for three different combinations, with the digital surface model corresponding to 01/08/2018 used as the reference DSM. In total, there were three subtractions: (a) one between the first and the second recording date, (b) one between the second and the third date, and (c) one between the first and the third date. The maximum positive DoD was 3.329 m and the maximum negative was 3.427 m. The DSMs that contributed to the process of subtraction and creation of digital model of difference relief had a spatial resolution of 8 cm. Finally, the above procedure was performed for both examined cartographic scales. Figure 9a illustrates the positive differences between two DSMs around windmills' bases for the time period of August through October 2018. By executing this subtraction, a petrified tree trunk was revealed at site 1. The geometric features of the trunk were measured precisely due to the ultra-high spatial resolution of the DSM. This specific trunk has a length of 9.7 m and a width of 0.4 m, and the total surface area excavated at this site was 204 m<sup>2</sup>. Figure 9b shows the result of the second subtraction, i.e., for the time period of October through November 2018, where intense excavation activity occurred. Significant negative elevation differences can be observed at the first site and three fossil trunks are easy to detect. One trunk is 3.8 m long and its width is 0.3 m, the second one has a length of 9.6 m and a width of 0.7 m, while the length of the third is 11 m and its width is 0.6 m. The total changes that occurred during the four-month long period (August to November 2018) of excavation works appear in Figure 9c. Intensive excavation activity was observed at the first site of wind turbine installation, where a total of four petrified tree trunks appeared. The DSM, which was used as the reference model, had a spatial resolution of 8 cm, as no lower altitude flight was made on the first recording date.

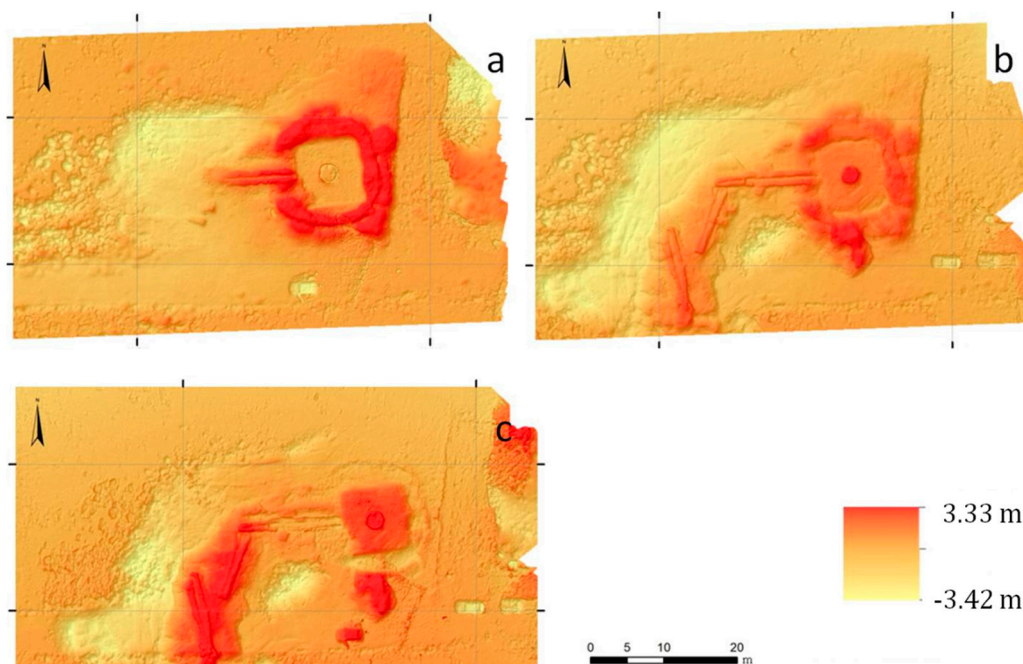


**Figure 9.** Map of changes with the DSM of difference method for site 1, (a) difference between 01 August 2018–07 October 2018, (b) difference between 07 October 2018–11 November 2018, and (c) difference between 01 August 2018–11 November 2018.

### 5. 3D Geovisualization

In this section, we present the 3D geovisualization methods used to create the augmented maps, along with the final cartographic list, which were both integrated into the mobile application. For the augmented 3D geovisualization, we used the two cartographic products we described previously; the DSM and the orthophotomap. The final 3D model was built by adding layers to the DSM. These layers were: (a) a grayscale displacement map containing height information, (b) a 3D Mesh, (c) 2D map images for texturing. The layers were assembled in this order on the DSM. This layering technique was used to create 3D models for each of the three large data recording scales used on the three dates of data recording. More precisely, as shown in Figure 10, three pairs of data were created, containing information about the altitude change between two recording dates. The visualization of the changes on the 3D model was achieved using a yellow–red color palette, where the red represented the sharp changes between two dates. These colors were chosen in order to avoid visual confusion and unnecessary information on the augmented map, as augmented reality already provides additional information, and the intersection of the functional with the unnecessary is subtle. Regarding the scale of the 3D models, it is proportional to the orthophotomap to which it corresponds and allows the observation of the position of the tree trunks, the altitude at which they were excavated, the 3D spatial variation of the study area, the spatial relationships between the trunks, and the levels of petrified tree trunks, as it allows the situation to be compared between dates.

The second method used for creating 3D models for later use in the mobile application was imaged-based 3D modeling. Using imaged-based 3D modeling, we were also able to create photorealistic models at the trench level for all three dates of data recording. Specifically, the 3D models derived from image-based 3D modeling provide photorealistic information about the actual texture of the fossils and the relief of the study area (Figure 11). The cartographic scale of the augmented map is 1:50, and the study area the user visualizes is the first site of installation. Each 3D model represents the study area at each of the recording dates (01/08/2018, 07/10/2018, and 11/11/2018). The spatial resolution of the models is very high, and the geometrical characteristics of the petrified tree trunks, the altitude excavated, and their slope and orientation can be discerned. Having the 3D models ready for use, we

then proceeded to match them with appropriate 2D AR markers to be projected onto when using AR. The orthophotomap of the first date was used as the target image in order to visualize all the changes through the AR. The AR application was built in the Unity 3D environment supported by the Vuforia software development kit (SDK). The final product was an Android mobile application (Figure 12) in which users can choose the information they want to experience in AR from the menu placed at the right of the screen, and also observe the changes between the days of data recording using the timeline menu at the bottom of the screen.



Figure 10. Android augmented reality (AR) application.

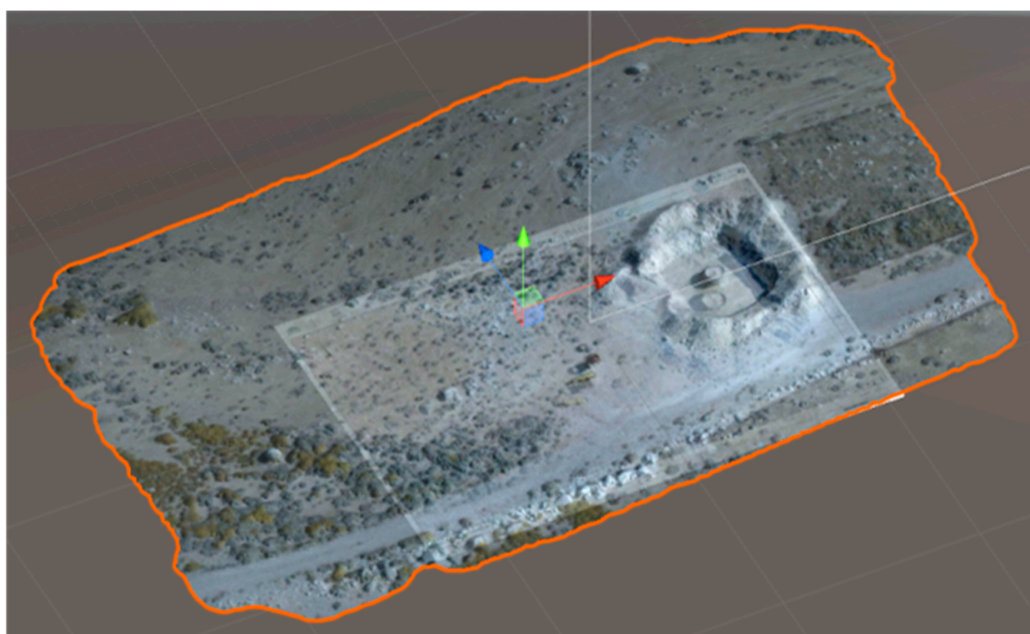
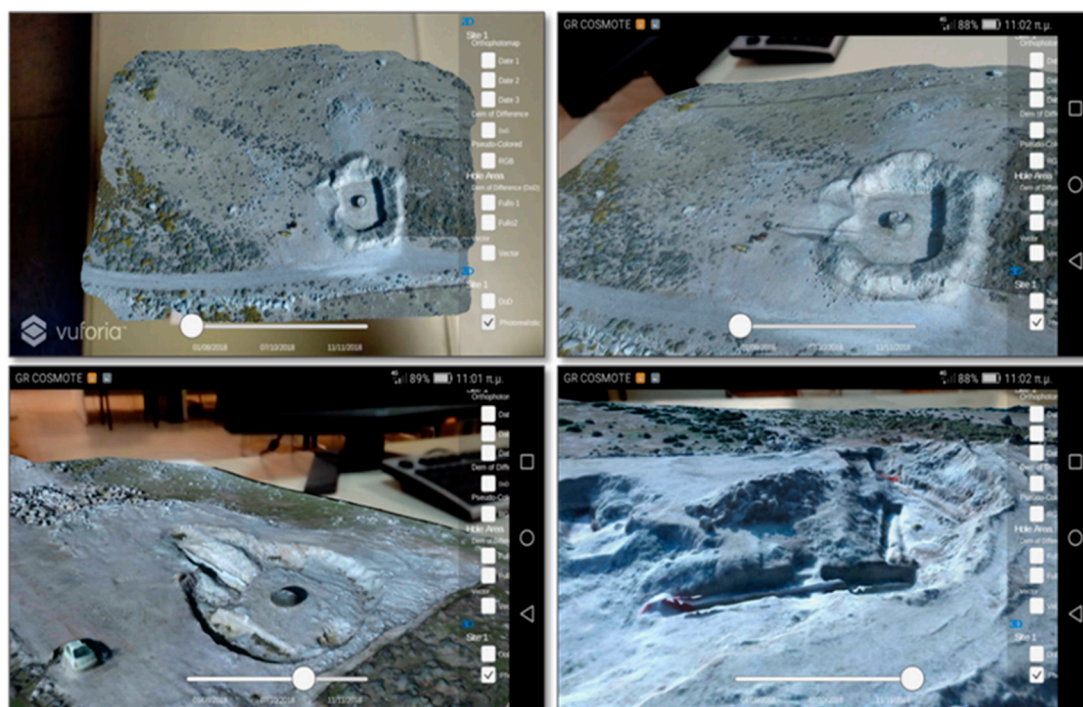


Figure 11. Three-dimensional model at the trench level at site 1, superimposed to the orthomosaic using AR marker in Unity 3D.



**Figure 12.** AR application at the trench level scale with photorealistic 3D geovisualization, at three recording dates.

## 6. Conclusions

During the construction of technical works within protected areas, geoconservation methodology is often required to provide the necessary protection and preservation for vulnerable geosites and, more specifically, fossil sites. The excavation process on a fossil site requires a monitoring methodology that will provide a complete and accurate overview of the fossils, their orientation, dimensions, and location within the different pyroclastic horizons, as well as the progress of the excavation works. This study proposes an AR application driven by the purpose of usability, providing advanced visualization of petrified tree trunk locations and information acquisition about their geometric characteristics easily and quickly. The interaction is between: (a) the mobile platform and the analogue map and (b) the user and the 3D digital space. The suggested methodology for monitoring excavation works was implemented at the Acroheiras Wind Park on Lesbos island, Greece, which is located in the Lesbos Petrified Forest, a protected natural monument. Concurrent processes, i.e., installation of new windmills and excavation of petrified tree trunks, were needed to be accomplished in a short time and with extra care due to the importance of fossil findings. Thus, the development of an application which collects data for both surveillance of the whole area and excavation trenches was considered necessary.

UAS data acquisition took place at three different time periods by capturing the entire study area at different altitudes. The aim was to gather a sufficient data set which would be capable of composing the desired cartographic derivatives. The latter data were used for building the AR environment of the application and were generated by processing of 4K video data. The choice of processing this type of data was made due to their high resolution and because they can fulfill the need for accurate and photorealistic 3D models, DSMs, and orthophotomaps. Regarding the drawbacks of UAS surveying for data acquisition, only the known limitation of poor weather conditions could be mentioned as a reason for not allowing flight missions. In our case, there was a temporal gap of a month due to severe winds that were blowing in the area, which interrupted our field work. The absence of dense and high vegetation in the surrounding area made it easier to represent the area's surface; otherwise, oblique UAS images together with terrestrial images should be applied so as to achieve the sufficient 3D model

with any blind spots. The proposed methodology introduces a new approach of geovisualization by making an application which combines three-dimensional (3D) and two-dimensional (2D) cartography with augmented reality (AR). A database with cartographic information at two scales helps the user either observe the whole excavation area or focus on petrified tree trunk features. The cartographic scale of 1:500 provides the opportunity for inspection of the wider area and the alterations of the environment that occurred during excavation works. However, the presence of the 1:50 scale is essential for thorough examination of the petrified tree trunks.

The AR application developed for mobile devices can be activated without any specialized software. It provides the ability to reproduce multi-feature data and thematic information in a 3D, augmented environment. The user can specify the time period of interest in order to visualize the changes. Finally, this AR application can be used by geoheritage specialists in their fieldwork, alongside excavation monitoring and geosite management. It also helps in gathering cartographic information and transferring it anywhere, allowing it to be used at any time. It supports multiple views of the same dataset, and therefore, it can be applied at a shared workspace. In addition, the inclusion of cartographic information with the database makes it easy for a user to retrieve the desired information, using the cartographic method that best serves them, depending on the object they want to observe. The AR tool also has limitations that could be addressed in the future. Existing mobile phone technology can visually render a specific number of faces of a 3D model. This means that if a 3D model of very high spatial analysis is created, the total area of which exceeds this number, it will not be able to be visualized with this technique. In conclusion, this study provides a framework which combines UAS image-based 3D modeling and AR technology for multitemporal monitoring of the excavation process of a geoheritage site. It can be stated that UASs provide data from which spatially accurate 3D information can be generated, which can be further exploited and geovisualized by AR applications for assisting management bodies and geoscientists.

**Author Contributions:** Conceptualization, Ermioni-Eirini Papadopoulou, Nikolaos Zouros and Nikolaos Soulakellis; Methodology, Ermioni-Eirini Papadopoulou; Software, Ermioni-Eirini Papadopoulou and Vlasios Kasapakis Writing-Original Draft Preparation, Ermioni-Eirini Papadopoulou and Apostolos Papakonstantinou; Writing-Review & Editing, All. All authors have read and agreed to the published version of the manuscript.

**Funding:** This research received no external funding.

**Conflicts of Interest:** The authors declare no conflict of interest.

## References

1. Goralski, R.; Gold, C. Marine GIS: Progress in 3D Visualization for Dynamic GIS. In *Lecture Notes in Geoinformation and Cartography*; Springer: Berlin/Heidelberg, Germany, 2008; pp. 401–416. ISBN 9783540685654.
2. Santos, I.; Henriques, R.; Mariano, G.; Pereira, D.I. Methodologies to Represent and Promote the Geoheritage Using Unmanned Aerial Vehicles, Multimedia Technologies, and Augmented Reality. *Geoheritage* **2018**, *10*, 143–155. [[CrossRef](#)]
3. Cayla, N.; Hobléa, F.; Reynard, E. New Digital Technologies Applied to the Management of Geoheritage. *Geoheritage* **2014**, *6*, 89–90. [[CrossRef](#)]
4. Lerma, J.L.; García, A. 3D City Modelling and Visualization of Historical Centers. In Proceedings of the CIPA Internacional Workshop of Vision Techniques applied to the Rehabilitation of City Centres, Lisbon, Portugal, 25–27 October 2004.
5. Niedzielski, T. Applications of Unmanned Aerial Vehicles in Geosciences: Introduction. *Pure Appl. Geophys.* **2018**, *175*, 3141–3144. [[CrossRef](#)]
6. Hatch, M. Environmental Geophysics. *Preview* **2017**, *2017*, 32–33. [[CrossRef](#)]
7. Clapuyt, F.; Vanacker, V.; Van Oost, K. Reproducibility of UAV-based earth topography reconstructions based on Structure-from-Motion algorithms. *Geomorphology* **2016**, *260*, 4–15. [[CrossRef](#)]
8. Westoby, M.J.; Brasington, J.; Glasser, N.F.; Hambrey, M.J.; Reynolds, J.M. “Structure-from-Motion” photogrammetry: A low-cost, effective tool for geoscience applications. *Geomorphology* **2012**, *179*, 300–314. [[CrossRef](#)]

9. De Reu, J. Image-Based 3D Modeling. In *The Encyclopedia of Archaeological Sciences*; John Wiley & Sons, Inc.: Hoboken, NJ, USA, 2018; pp. 1–4.
10. Dellepiane, M.; Dell’Unto, N.; Callieri, M.; Lindgren, S.; Scopigno, R. Archeological excavation monitoring using dense stereo matching techniques. *J. Cult. Herit.* **2013**, *14*, 201–210. [[CrossRef](#)]
11. Peng, F.; Lin, S.C.; Guo, J.; Wang, H.; Gao, X. The Application of SfM Photogrammetry Software for Extracting Artifact Provenience from Palaeolithic Excavation Surfaces. *J. Field Archaeol.* **2017**, *42*, 326–336. [[CrossRef](#)]
12. Kasprzak, M.; Jancewicz, K.; Michniewicz, A. UAV and SfM in Detailed Geomorphological Mapping of Granite Tors: An Example of Starościńskie Skały (Sudetes, SW Poland). *Pure Appl. Geophys.* **2018**, *175*, 3193–3207. [[CrossRef](#)]
13. Jo, Y.; Hong, S. Three-Dimensional Digital Documentation of Cultural Heritage Site Based on the Convergence of Terrestrial Laser Scanning and Unmanned Aerial Vehicle Photogrammetry. *ISPRS Int. J. Geo-Inf.* **2019**, *8*, 53. [[CrossRef](#)]
14. Azuma, R.T. A Survey of Augmented Reality. *Presence Teleoperators Virtual Environ.* **1997**, *6*, 355–385. [[CrossRef](#)]
15. Kim, W.; Kerle, N.; Gerke, M. Mobile augmented reality in support of building damage and safety assessment. *Nat. Hazards Earth Syst. Sci.* **2016**, *16*, 287–298. [[CrossRef](#)]
16. Kamat, V.R.; El-Tawil, S. Evaluation of Augmented Reality for Rapid Assessment of Earthquake-Induced Building Damage. *J. Comput. Civ. Eng.* **2007**, *21*, 303–310. [[CrossRef](#)]
17. Siekański, P.; Michoński, J.; Bunsch, E.; Sitnik, R. CATCHA: Real-Time Camera Tracking Method for Augmented Reality Applications in Cultural Heritage Interiors. *ISPRS Int. J. Geo-Inf.* **2018**, *7*, 479. [[CrossRef](#)]
18. Panou, C.; Ragia, L.; Dimelli, D.; Mania, K. An Architecture for Mobile Outdoors Augmented Reality for Cultural Heritage. *ISPRS Int. J. Geo-Inf.* **2018**, *7*, 463. [[CrossRef](#)]
19. Bertok, C.; Lozar, F.; Magagna, A.; Giordano, E.; D’Atri, A.; Dela Pierre, F.; Natalicchio, M.; Martire, L.; Clari, P.; Violanti, D.; et al. Virtual Tours Through Earth’s History and Palaeoclimate: Examples from the Piemonte (Northwestern Italy) Geoheritage (PROGEO-Piemonte Project). In *Springer Geology*; Springer: Cham, Switzerland, 2014; pp. 299–302.
20. Rapprich, V.; Lisec, M.; Fiferna, P.; Závada, P. Application of Modern Technologies in Popularization of the Czech Volcanic Geoheritage. *Geoheritage* **2017**, *9*, 413–420. [[CrossRef](#)]
21. Martínez-Graña, A.; González-Delgado, J.Á.; Ramos, C.; Gonzalo, J.C. Augmented Reality and Valorizing the Mesozoic Geological Heritage (Burgos, Spain). *Sustainability* **2018**, *10*, 4616. [[CrossRef](#)]
22. Zollmann, S.; Hoppe, C.; Kluckner, S.; Poglitsch, C.; Bischof, H.; Reitmayr, G. Augmented Reality for Construction Site Monitoring and Documentation. *Proc. IEEE* **2014**, *102*, 137–154. [[CrossRef](#)]
23. Koo, S.; Kim, J.; Kim, C.; Kim, J.; Cha, H.S. Development of an Augmented Reality Tour Guide for a Cultural Heritage Site. *J. Comput. Cult. Herit.* **2020**, *12*, 1–24. [[CrossRef](#)]
24. Koufos, G.D.; Zouros, N.; Mourouzidou, O. *Prodeinotherium bavaricum* (Proboscidea, Mammalia) from Lesvos island, Greece; the appearance of deinotheres in the eastern Mediterranean. *Geobios* **2003**, *36*, 305–315. [[CrossRef](#)]
25. Vasileiadou, K.; Böhme, M.; Neubauer, T.A.; Georgalis, G.L.; Syrides, G.E.; Papadopoulou, L.; Zouros, N. Early Miocene gastropod and ectothermic vertebrate remains from the Lesvos Petrified Forest (Greece). *PalZ* **2017**, *91*, 541–564. [[CrossRef](#)]
26. Zouros, N.C. The Petrified Forest of Lesvos A Unique Natural Monument. In *Natural Heritage from East to West*; Springer: Berlin/Heidelberg, Germany, 2010; pp. 15–26. ISBN 9783642015762.
27. Soulakellis, N.; Tataris, G.; Papadopoulou, E.-E.; Chatzistamatis, S.; Vasilakos, C.; Kavroudakis, D.; Roussou, O.; Papakonstantinou, A. Synergistic Exploitation of Geoinformation Methods for Post-earthquake 3D Mapping and Damage Assessment. In *Lecture Notes in Geoinformation and Cartography*; Springer: Cham, Switzerland, 2019; pp. 3–31. ISBN 9783030053291.
28. Agisoft LLC Agisoft PhotoScan User Manual: Professional Edition, Version 1.2. Available online: [https://www.agisoft.com/pdf/photoscan-pro\\_1\\_2\\_en.pdf](https://www.agisoft.com/pdf/photoscan-pro_1_2_en.pdf) (accessed on 14 May 2020).

